arXiv:1604.06081v1 [quant-ph] 20 Apr 2016

Characteristic properties of the Casimir free energy for metal films deposited on metallic plates

G. L. Klimchitskaya[1,2] and V. M. Mostepanenko[1,2]

[1]*Central Astronomical Observatory at Pulkovo of the Russian Academy of Sciences, Saint Petersburg, 196140, Russia*

[2]*Institute of Physics, Nanotechnology and Telecommunications, Peter the Great Saint Petersburg Polytechnic University, St.Petersburg, 195251, Russia*

Abstract

The Casimir free energy and pressure of thin metal films deposited on metallic plates are considered using the Lifshitz theory and the Drude and plasma model approaches to the role of conduction electrons. The bound electrons are taken into account by using the complete optical data of film and plate metals. It is shown that for films of several tens of nanometers thickness the Casimir free energy and pressure calculated using these approaches differ by hundreds and thousands percent and can be easily discriminated experimentally. According to our results, the free energy of a metal film does not vanish in the limiting case of ideal metal if the Drude model approach is used in contradiction with the fact that the fluctuating field cannot penetrate in its interior. Numerical computations of the Casimir free energy and pressure of Ag and Au films deposited on Cu and Al plates have been performed using both theoretical approaches. It is shown that the free energy of a film can be both negative and positive depending on the metals used. For a Au film on a Ag plate and vice versa the Casimir energy of a film changes its sign with increasing film thickness. Applications of the obtained results for resolving the Casimir puzzle and the problem of stability of thin films are discussed.

PACS numbers: 12.20.Ds, 42.50.Lc, 78.20.-e

I. INTRODUCTION

It is well known that the van der Waals and Casimir energies and forces arise between two closely spaced material bodies due to the zero-point and thermal fluctuations of the electromagnetic field [1, 2]. During the last few years the Casimir effect has found numerous applications in atomic physics [3–7], condensed matter physics [8–12] and nanotechnology [13–15] (see also reviews [16, 17]). The high-tech laboratory setups using an atomic force microscope [16] and a micromechanical torsional oscillator [17] made possible measuring the Casimir interaction with unprecedented precision. This has opened up opportunities for quantitative comparison of the experimental data with theoretical predictions of the Lifshitz theory [1, 2, 18], which provides a unified fundamental description of both the van der Waals and Casimir forces on the basis of first principles of quantum electrodynamics and quantum statistical physics.

The Lifshitz theory represents the van der Waals and Casimir free energies and forces as some functionals of the frequency-dependent dielectric permittivities and magnetic permeabilities of interacting bodies. In so doing, the dielectric permittivities in common use include the contributions from both free and bound charge carriers (electrons for metals). A comparison between the experimental data of all precise experiments on measuring the Casimir force performed for metallic test bodies [19–25] with the predictions of the Lifshitz theory has revealed a problem, the so-called Casimir puzzle. It turned out that if the relaxation properties of free (conduction) electrons are taken into account in calculations (this is usually done by using the Drude model), the theoretical results are excluded by the measurement data at up to 99% confidence level [19–25]. By contrast, if the relaxation properties of free electrons are omitted (i.e., the free charge carriers are described by the nondissipative plasma model), the measurement data are found in agreement with theoretical predictions at more than 90% confidence level [26]. These results are puzzling because the major difference in theoretical predictions of both models comes from the zero-frequency term of the Lifshitz formula, where, according to common views, the role of dissipation is rather large and should be taken into account.

The above puzzle gave rise to a long-term discussion in the literature, where a lot of arguments pro and contra of using the Drude and plasma dielectric permittivities in the Lifshitz theory has been proposed (see, e.g., Refs. [27–34]). It should be noted that at

separation distances below $1\,\mu$m, where the magnitude of the Casimir force is large enough to be measured with high precision, the difference in theoretical predictions using the Drude and plasma models does not exceed a few percent. In spite of the fact that the experimental precision was equal to a fraction of a percent, this gave grounds for attempted explanations of a puzzle by the role of some unaccounted background effects, e.g., by the influence of patch potentials [35] (thereafter the role of this effect in the test bodies of Refs. [19–22] was shown to be negligibly small [36]).

An experimental situation has become conclusively established after the difference force measurement was performed [38**?**], where theoretical predictions of the Drude and plasma models differ by a factor of a few hundreds. The results of this experiment, which was proposed in Refs. [39–41], excluded the predictions of the Drude model and are consistent with the plasma model [38]. Several experiments using dielectric and dielectric-type semiconductor test bodies [6, 42–44] are also worthy of notice. The measurement data of these experiments exclude the predictions of the Lifshitz theory obtained with taken into account contribution of free charge carriers (dc conductivity), and are consistent with the same theory if the free charge carriers are omitted [6, 42–45]. It is significant that the Lifshitz theory violates the third law of thermodynamics (the Nernst heat theorem) if it describes conduction electrons in metals with perfect crystal lattices by means of the Drude model [46–49] or takes into account the free charge carriers in dielectrics [50–53]. By contrast, if the plasma model is used for metals and the free charge carriers are omitted for dielectrics, the Lifshitz theory is found in perfect agreement with the Nernst heat theorem [46–53].

As was shown recently in Ref. [54], the Lifshitz theory using the Drude and plasma models predicts significantly different values of the Casimir free energy and pressure for a metallic film either sandwiched between two dielectric plates or in vacuum. These configurations have some advantages, as compared with difference force measurements [38–41], because in the case of the plasma model the latter result in a detectable but rather small signal of the order of 0.1 pN. It was found also that when the Drude model is used the Casimir free energy does not vanish in the limiting case of ideal metal in contradiction with the fact that electromagnetic oscillations cannot penetrate in its interior.

In this paper, we investigate the Casimir free energy and pressure for metal films deposited on metallic plates using the Lifshitz theory and describing the conduction electrons by both the Drude and plasma models. The interest to this subject is twofold. On the one hand, the

configuration of two dissimilar metallic layers is analogous to that considered in Ref. [54]. Thus, one may expect significantly different values of the Casimir free energy and pressure when the Drude and plasma models are employed in calculations for experimentally used film thicknesses. On the other hand, the obtained results are helpful to determine the role of van der Waals and Casimir forces in stability of thin films, which is the problem important for numerous applications [55].

We calculate the Casimir free energy and pressure for Au and Ag films deposited on the plates made of different metals. All calculations are done using the Drude and plasma models for the description of conduction (free) electrons. The contribution of core (bound) electrons is taken into account by means of the tabulated optical data. It is shown that the Casimir free energy of a film can be negative, positive or change its sign as a function of film thickness depending on the film and plate metals. We demonstrate that even for thin films of several tens of nanometers thickness the Casimir free energy and pressure computed using the Drude and plasma model approaches can differ by hundreds and thousands percent. This result is important for resolving the Casimir puzzle formulated above.

One more qualitative result is that the Casimir free energy of metal film on a metallic plate reaches the classical limit for rather small film thickness of about 150 nm and only if the Drude model is used for the theoretical description of free electrons. If the plasma model is used for this purpose, the free energy drops exponentially fast to zero with increasing film thickness, and there is no classical limit. Because of this, starting from rather small film thicknesses, the use of optical data leads to only minor influence on the computational results obtained by using the simple Drude model. For thin films, however, the optical data contribute essentially, especially if the Casimir energy of a film changes its sign. We show that in the framework of the plasma model approach the optical data should be taken into account for films of any thickness. It is shown also that the free energy of a metal film does not vanish in the ideal metal limit if the Drude model is used.

The paper is organized as follows. Section II presents general formalism of the Lifshitz theory for metal films deposited on metallic plates and some analytic results. In Sec. III the computational results using the tabulated optical data and the Drude and plasma models are presented for the film and plate metals leading to the negative free energies and pressures. In Sec. IV similar results are given for the film and plate metals leading to the positive free energies and pressures. Section V is devoted to cases where the Casimir free energy changes

its sign. Section VI contains our conclusions and discussion.

II. GENERAL FORMALISM FOR TWO-LAYER METALLIC SYSTEM

The case of a two-layer system is most simply obtained from the three-layer case when one of the dielectric permittivities is put equal to unity. Let the dielectric permittivities of a thick metallic plate (semispace) and deposited on it metal film of thickness a be $\varepsilon^{(1)}(\omega)$ and $\varepsilon^{(2)}(\omega)$, respectively. The third (thick) layer we replace with a vacuum and put $\varepsilon^{(3)}(\omega) = 1$. Assuming that out two-layer system is in thermal equilibrium with an environment at temperature T, for the Casimir free energy of a metal film per unit area one obtains [2, 18, 54]

$$\mathcal{F}(a,T) = \frac{k_B T}{2\pi}{\sum_{l=0}^{\infty}}' \int_0^{\infty} k_\perp \, dk_\perp \sum_\alpha \ln\left[1 - r_\alpha^{(2,3)}(i\xi_l, k_\perp) r_\alpha^{(2,1)}(i\xi_l, k_\perp) e^{-2a k_l^{(2)}(k_\perp)}\right]. \tag{1}$$

Here, k_B is the Boltzmann constant, $\xi_l = 2\pi k_B T l/\hbar$ with $l = 0, 1, 2, \ldots$ are the Matsubara frequencies, $k_\perp = |\boldsymbol{k}_\perp|$ is the magnitude of the projection of the wave vector on the plane of plates, the prime adds a multiple 1/2 to the term with $l = 0$, and the second summation is made over two independent polarizations of the electromagnetic field, transverse magnetic ($\alpha = \mathrm{TM}$) and transverse electric ($\alpha = \mathrm{TE}$). The respective reflection coefficients are given by

$$r_{\mathrm{TM}}^{(2,n)}(i\xi_l, k_\perp) = \frac{\varepsilon_l^{(n)} k_l^{(2)}(k_\perp) - \varepsilon_l^{(2)} k_l^{(n)}(k_\perp)}{\varepsilon_l^{(n)} k_l^{(2)}(k_\perp) + \varepsilon_l^{(2)} k_l^{(n)}(k_\perp)}, \quad r_{\mathrm{TE}}^{(2,n)}(i\xi_l, k_\perp) = \frac{k_l^{(2)}(k_\perp) - k_l^{(n)}(k_\perp)}{k_l^{(2)}(k_\perp) + k_l^{(n)}(k_\perp)}, \tag{2}$$

where $n = 1, 2, 3$ and the following notation is introduced:

$$k_l^{(n)}(k_\perp) = \sqrt{k_\perp^2 + \varepsilon_l^{(n)} \frac{\xi_l^2}{c^2}} \tag{3}$$

and $\varepsilon_l^{(n)} \equiv \varepsilon^{(n)}(i\xi_l)$.

From Eq. (1) for the Casimir pressure on a metallic film one obtains

$$P(a,T) = -\frac{k_B T}{\pi}{\sum_{l=0}^{\infty}}' \int_0^{\infty} k_\perp k_l^{(2)}(k_\perp) \, dk_\perp \sum_\alpha \left[\frac{e^{2a k_l^{(2)}(k_\perp)}}{r_\alpha^{(2,3)}(i\xi_l, k_\perp) r_\alpha^{(2,1)}(i\xi_l, k_\perp)} - 1\right]^{-1}. \tag{4}$$

Taking into account the present state of affairs (see Sec. I), we describe the dielectric permittivities of the film and plate metals by the Drude or plasma model (the bound electrons are taken into account in numerical computations of Secs. III–V). The dielectric permittivity of the Drude model at real and imaginary Matsubara frequencies takes the form

$$\varepsilon_D^{(n)}(\omega) = 1 - \frac{\omega_{p,n}^2}{\omega(\omega + i\gamma_n)}, \quad \varepsilon_{l,D}^{(n)} = 1 + \frac{\omega_{p,n}^2}{\xi_l(\xi_l + \gamma_n)}, \tag{5}$$

where $\omega_{p,n}$ are the plasma frequencies of the film ($n=2$) and plate ($n=1$) metals and γ_n are their relaxation frequencies (the latter are temperature-dependent, and all computations below are performed at room temperature $T=300\,\mathrm{K}$). The dielectric permittivity of the plasma model is obtained from Eq. (5) by putting $\gamma_n=0$

$$\varepsilon_p^{(n)}(\omega)=1-\frac{\omega_{p,n}^2}{\omega^2},\quad \varepsilon_{l,p}^{(n)}=1+\frac{\omega_{p,n}^2}{\xi_l^2}, \tag{6}$$

Note that both dielectric functions (5) and (6) can be analytically continued to the entire plane of complex frequencies and satisfy the Kramers-Kronig relations formulated for the functions having the first- and second-order poles at zero frequency, respectively [56].

We start from the zero-frequency contribution to Eqs. (1) and (4). In the case of the Drude model (5), from Eq. (2) one finds

$$r_{\mathrm{TM},D}^{(2,3)}(0,k_\perp)=-1,\quad r_{\mathrm{TE},D}^{(2,n)}(0,k_\perp)=0,\quad r_{\mathrm{TM},D}^{(2,1)}(0,k_\perp)=\frac{\omega_{p,1}^2\gamma_2-\omega_{p,2}^2\gamma_1}{\omega_{p,1}^2\gamma_2+\omega_{p,2}^2\gamma_1}\equiv r_D^{(0)}. \tag{7}$$

As is seen in Eq. (7), these reflection coefficients do not depend on $k_\perp$ and $|r_D^{(0)}|\ll 1$. Note that the quantity $r_D^{(0)}$ may be both positive and negative depending on the relationship between the Drude parameters of a film and a plate metals. Substituting Eq. (7) in Eq. (1), for the zero-frequency contribution to the Casimir free energy calculated using the Drude model we have

$$\mathcal{F}_D^{(l=0)}(a,T)=\frac{k_BT}{4\pi}\int_0^\infty k_\perp dk_\perp\ln\left(1+r_D^{(0)}e^{-2ak_\perp}\right). \tag{8}$$

Introducing the new dimensionless integration variable $y=2ak_\perp$, one arrives at

$$\mathcal{F}_D^{(l=0)}(a,T)=\frac{k_BT}{16\pi a^2}\int_0^\infty ydy\ln\left(1+r_D^{(0)}e^{-y}\right)=-\frac{k_BT}{16\pi a^2}\mathrm{Li}_3(-r_D^{(0)}), \tag{9}$$

where $\mathrm{Li}_n(z)$ is the polylogarithm function. Depending on the sign of $r_D^{(0)}$, the zero-frequency contribution to the free energy is either positive or negative, i.e., corresponds to either repulsive or attractive contribution to the force. Using the smallness of $r_D^{(0)}$, we can represent Eq. (9) in the form of a series

$$\mathcal{F}_D^{(l=0)}(a,T)=\frac{k_BT}{16\pi a^2}r_D^{(0)}\left[1-\frac{1}{8}r_D^{(0)}+\frac{1}{27}(r_D^{(0)})^2-\ldots\right]. \tag{10}$$

Substituting Eq. (7) in Eq. (4) and repeating similar calculation, for the zero-frequency contribution to the Casimir pressure we find

$$P_D^{(l=0)}(a,T)=-\frac{k_BT}{8\pi a^3}\mathrm{Li}_3(-r_D^{(0)})=r_D^{(0)}\frac{k_BT}{8\pi a^3}\left[1-\frac{1}{8}r_D^{(0)}+\frac{1}{27}(r_D^{(0)})^2-\ldots\right]. \tag{11}$$

According to Ref. [54], the contribution of Matsubara terms with $l \geq 1$ to the Casimir free energy of a metal film sandwiched between two dielectric plates is negligibly small for surprisingly thin films if the film metal is described by the Drude model. By repeating the same calculation in our case of a metal film deposited on a metallic plate, we find that the contribution of all Matsubara terms with $l \geq 1$ becomes negligibly small for film thickness $a > 150\,\mathrm{nm}$. For these film thicknesses Eqs. (9)–(11) represent the total Casimir free energy and pressure, i.e., the classical limit is already achieved (recall that in the configuration of two metallic plates separated with a dielectric film the classical limit is achieved only at separations exceeding $6\,\mu\mathrm{m}$ [2]).

Now we consider the Casimir free energy and pressure $\mathcal{F}_D$ and P_D in the limiting case $\omega_{p,2} \to \infty$. This means that the dielectric permittivity of a metal film becomes infinitely large at all frequencies, i.e., its material is the so-called ideal metal. From Eqs. (3) and (5) we conclude that all $k_l^{(2)}(k_\perp)$ with $l \geq 1$ go to infinity when $\omega_{p,2} \to \infty$. Thus, according to Eqs. (1) and (4), only the zero-frequency Matsubara terms contribute to the free energy and pressure in this limiting case. Using Eq. (7) we find that $r_D^{(0)} \to -1$ when $\omega_{p,2} \to \infty$. Then, from Eqs. (9) and (11) one obtains

$$\mathcal{F}_D(a,T) = -\frac{k_B T}{16\pi a^2}\zeta(3), \quad P_D(a,T) = -\frac{k_B T}{8\pi a^3}\zeta(3), \tag{12}$$

where $\zeta(z)$ is the Riemann zeta function. The results (12) mean that an ideal metal film is characterized by a nonzero Casimir free energy and pressure if the Drude model is used in calculations. This is paradoxical if to take into account that electromagnetic fluctuations cannot penetrate in the interior of ideal metal.

If metals of a film and a plate are described by the plasma model (6), one arrives at quite different results. Substituting Eq. (6) in the first line of Eq. (2), the TM reflection coefficients at zero Matsubara frequency take the form

$$r_{\mathrm{TM},p}^{(2,1)}(0,k_\perp) = \frac{(\omega_{p,1}^2-\omega_{p,2}^2)[c^2k_\perp^2(\omega_{p,1}^2+\omega_{p,2}^2)+\omega_{p,1}^2\omega_{p,2}^2]}{(\omega_{p,1}^2\sqrt{c^2k_\perp^2+\omega_{p,2}^2}+\omega_{p,2}^2\sqrt{c^2k_\perp^2+\omega_{p,1}^2})^2}, \quad r_{\mathrm{TM},p}^{(2,3)}(0,k_\perp) = -1. \tag{13}$$

It can be seen that $r_{\mathrm{TM},p}^{(2,1)}$ is positive for $\omega_{p,1} > \omega_{p,2}$ and negative for $\omega_{p,1} < \omega_{p,2}$. From the

second line of Eq. (2) we have

$$r^{(2,1)}_{\mathrm{TE},p}(0,k_\perp)=\frac{\omega^2_{p,2}-\omega^2_{p,1}}{(\sqrt{c^2k^2_\perp+\omega^2_{p,2}}+\sqrt{c^2k^2_\perp+\omega^2_{p,1}})^2},$$
$$r^{(2,3)}_{\mathrm{TE},p}(0,k_\perp)=\frac{\omega^2_{p,2}}{(\sqrt{c^2k^2_\perp+\omega^2_{p,2}}+ck_\perp)^2}. \tag{14}$$

As is seen in Eq. (14), $r^{(2,1)}_{\mathrm{TE},p}>0$ when $\omega_{p,2}>\omega_{p,1}$ and $r^{(2,1)}_{\mathrm{TE},p}<0$ when $\omega_{p,2}<\omega_{p,1}$, whereas the reflection coefficient $r^{(2,3)}_{\mathrm{TE},p}$ is always positive. The above results open possibilities for both positive and negative Casimir free energy.

By repeating calculations of Ref. [54], it can be proven that the Casimir free energy (1) and pressure (4) with increasing film thickness a are expressed via the exponentially small terms depending on the Planck constant $\hbar$. Thus, there is no classical limit in the configuration of a metal film deposited on a metallic plate if the plasma model is used in calculations.

In the limiting case of an ideal metal film ($\omega_{p,2}\to\infty$) from Eq. (3) one finds

$$k^{(2)}_l(k_\perp)=\sqrt{k^2_\perp+\frac{\xi^2_l}{c^2}+\frac{\omega^2_{p,2}}{c^2}}\to\infty \tag{15}$$

for all $l\geq 0$. Then, from Eqs. (1) and (4) we obtain

$$\mathcal{F}(a,T)\to 0,\quad P(a,T)\to 0, \tag{16}$$

as it should be in accordance to physical intuition. Below we consider all the above general properties for several specific metals of a film and a plate.

III. FILMS WITH NEGATIVE CASIMIR FREE ENERGY

Here, we compute the Casimir free energy and pressure for Ag and Au films deposited on Cu plates using Eqs. (1)–(4). The dielectric permittivities of these metals at the imaginary Matsubara frequencies are obtained by means of the Kramers-Kronig relations using the tabulated optical data [57] extrapolated to zero frequency either by the Drude of by the plasma models (the Drude and plasma model approaches, respectively). In the case of Au such extrapolations with the plasma frequency $\omega_{p,\mathrm{Au}}=9.0\,\mathrm{eV}$ and relaxation parameter $\gamma_{\mathrm{Au}}=0.035\,\mathrm{eV}$ have been considered in detail and extensively used in calculations of the

Casimir force and comparison with the experimental data [2, 16]. For Ag the optical data [57] extend over the same frequency interval as for Au, i.e., from 0.125 to 10^4 eV, and the Drude parameters of the extrapolation are $\omega_{p,\mathrm{Ag}} = 9.66\,\mathrm{eV}$ and $\gamma_{\mathrm{Ag}} = 0.0315\,\mathrm{eV}$ in agreement with Ref. [58]. For Cu the optical data [57] extend from 0.13 to 9×10^3 eV and similar extrapolation to lower frequencies results in $\omega_{p,\mathrm{Cu}} = 8.6\,\mathrm{eV}$ and $\gamma_{\mathrm{Cu}} = 0.0325\,\mathrm{eV}$. These results are rather close to the Drude parameter of Cu in Refs. [59, 60]. Taking into account that for all three metals the tabulated optical data extend up to sufficiently high frequencies, there is no need in further interpolations.

In Fig. 1(a) we present the computational results for the magnitude of the Casimir free energy per unit area of a Ag film deposited on a Cu plate as a function of film thickness a at $T = 300\,\mathrm{K}$ (all subsequent calculations are also performed at room temperature). Computations are performed over the range of a from 20 to 200 nm. Note that for $a > 10\,\mathrm{nm}$ one can neglect by the effect of anisotropy of atomically thin planar layers [61, 62]. The solid and dashed lines labeled 1 are computed using the optical data of both Ag and Cu extrapolated by the Drude model and the simple Drude model (5), respectively. The solid and dashed lines labeled 2 are calculated using the optical data of both Ag and Cu extrapolated by the plasma model and the simple plasma model (6), respectively.

According to our computational results, the Casimir free energy of Ag films on a Cu plate is always negative, i.e., the respective forces are attractive. Below we demonstrate that this result is not universal, so that the sign of $\mathcal{F}$ depends on the metals of a film and a plate and on the film thickness. As can be seen in Fig. 1(a), the magnitudes of the Casimir free energy calculated using the optical data extrapolated by the Drude and plasma models are significantly different. Thus, for Ag films of 50 and 100 nm thickness the Casimir free energies predicted by the Drude and plasma model approaches differ by the factors of 2.76 and 156.6, respectively. With increasing film thickness a the difference in theoretical predictions of both approaches further increases. This is explained by the exponentially fast vanishing of the Casimir free energy calculated using the plasma model approach (see the solid line 2), whereas $\mathcal{F}_D$ (the solid line 1) goes to the classical limit (9). We remind that in the configuration of two metallic plates separated with a vacuum gap of width a the difference in theoretical predictions of the Drude and plasma model approaches at $a < 1\,\mu\mathrm{m}$ is below a few percent and reaches 100% only at $a = 6\,\mu\mathrm{m}$ [2, 16].

We also note on the role of optical data in both calculation approaches. As is seen in

Fig. 1(a), an influence of the optical data on computational results is much larger in the plasma model approach than in the Drude model one. Thus, for the films of 50 and 100 nm thickness the simple Drude model (the dashed line 1) leads to by the factors 1.52 and 1.01 larger results, respectively, than the optical data extrapolated by the Drude model (the solid line 1). For the plasma model approach the respective factors found from a comparison of the dashed and solid lines 2 are 2.30 and 2.31, and they do not decrease with increasing a. This is explained by the fact that for the plasma model approach the relative role of the zero-frequency term (which does not depend on the optical data) decreases with increasing film thickness. For two metallic plates separated with a vacuum gap the Casimir free energy is always negative, and the magnitudes of the Casimir free energy computed using the optical data are larger than using the simple Drude or plasma models. In that case the optical data do not influence as strong as for a metal film on a metallic plate. Thus, for a Ag plate interacting with a Cu plate at separations 50 and 100 nm an excess of $|\mathcal{F}|$ due to the use of optical data is by the factors of 1.094 and 1.037 for the Drude model and of 1.097 and 1.038 for the plasma model, respectively.

In Fig. 1(b) the solid and dashed lines labeled 1 present the Casimir pressure in a Ag film computed using the optical data extrapolated by the Drude model and the simple Drude model, respectively, as a function of the film thickness. The solid and dashed lines labeled 2 show similar results computed using the plasma model. As is seen in Fig. 1(b), the Casimir pressure behaves analogously to the free energy. Thus, the role of optical data is more pronounced in the plasma model approach than in the Drude model one. With increasing a the Casimir pressure computed using the plasma model exponentially fast drops to zero, i.e., there is no classical limit. For the Drude model approach the classical limit (11) is already achieved for films of 150 nm thickness. Similar to the case of the free energy, the Casimir pressures calculated using the Drude and plasma model approaches are significantly different even for Ag films of 50 and 100 nm thickness.

For a Ag film deposited on a Cu plate the respective plasma frequencies satisfy an inequality $\omega_{p,\mathrm{Ag}} > \omega_{p,\mathrm{Cu}}$. One more example of this kind is presented by a Au film deposited on a Cu substrate. The magnitude of the Casimir free energy of this film computed using the tabulated optical data extrapolated by the Drude and plasma models are shown in Fig. 2 as functions of film thickness by the solid lines labeled 1 and 2, respectively. The dashed lines 1 and 2 are computed using the simple Drude and plasma models, respectively. Similar to

the case of a Ag film on a Cu plate, the free energy of a Au film is negative. The classical limit is reached for Au films of about 150 nm thickness if the Drude model approach is used. There is no classical limit in the plasma model approach. As is seen in Fig. 2, for films of 50 and 100 nm thickness the magnitudes of the free energy computed using the optical data and the Drude model are by the factors of 1.15 and 16.6 larger than those computed using the optical data and the plasma model, respectively. These factors are smaller than for a Ag film but still much larger than for two metallic plates interacting through a vacuum gap. The role of optical data in the Drude model approach decreases with increasing film thickness. For instance, for films of 50 and 100 nm thickness the magnitudes of the free energy computed using the simple Drude model are larger by the factors of 1.76 and 1.10 than those computed using the optical data, respectively. For the plasma model approach the respective factors are 1.84 and 2.50 for the same film thicknesses. Here, the role of optical data does not decrease with increasing film thickness.

IV. FILMS WITH POSITIVE CASIMIR FREE ENERGY

Unlike the case of two metallic plates interacting through a vacuum gap, the free energy and pressure of a metal film deposited on a metallic plate can be positive. Here, we consider Au and Ag films on an Al plate. The tabulated optical data for Al over the frequency range from 0.04 to 10^4 eV were taken in Ref. [57] and extrapolated to zero frequency by the Drude or plasma models with the parameters $\omega_{p,\mathrm{Al}} = 11.34\,\mathrm{eV}$ and $\gamma_{\mathrm{Al}} = 0.041\,\mathrm{eV}$ in rather good agreement with Ref. [63]. Then the dielectric permittivity of Al at the imaginary Matsubara frequencies using the Drude and plasma model approaches was found as described in Refs. [2, 16]. For the films considered in this section the plasma frequencies are less than the plasma frequency of the plate. This makes possible the effect of the Casimir repulsion.

In Fig. 3(a) the solid and dashed lines labeled 1 present the Casimir free energy per unit area of a Au film on an Al plate computed as a function of film thickness using the optical data and the Drude model (the solid line) and the simple Drude model (the dashed line). Similar results computed using the optical data and the plasma model or the simple plasma model are shown by the solid and dashed lines labeled 2, respectively. In Fig. 3(b) the computational results for the Casimir pressure of a Au film on an Al plate are presented using the same notations. As is seen in Fig. 3(a,b), the Casimir free energy and pressure of

a Au film in this case are positive which corresponds to the effect of repulsion. In the same manner as in Figs. 1 and 2, the Drude and plasma model approaches predict significantly different Casimir free energies (the solid lines 1 and 2). For film thicknesses of 50 and 100 nm these predictions differ by the factors of 1.52 and 30.6, respectively. With further increase of the film thickness the difference in theoretical predictions reaches several orders of magnitude. This is again explained by the exponentially fast decreasing of the Casimir free energy and pressure when the plasma model approach is used, whereas in the framework of the Drude model approach both these quantities reach the classical limit for film thicknesses of about 150 nm. The role of optical data in Fig. 3 is evidently smaller than in Figs. 1 and 2. For the dashed and solid lines labeled 1 (computed using the simple Drude model and the optical data extrapolated by the Drude model) the ratio of respective free energies for $a = 50\,\mathrm{nm}$ is equal to 1.057 and unity for $a = 100\,\mathrm{nm}$. For the dashed and solid lines labeled 2 (computed using the simple plasma model and the optical data extrapolated by the plasma model) the respective ratios take the values 1.094 and 1.234. Similar results are obtained for the Casimir pressure.

One more example of the positive Casimir free energy is given by a Ag film deposited on an Al plate. In this case the Casimir free energy calculated using the Drude and plasma model approaches is presented in Fig. 4 as a function of film thickness by the solid lines 1 and 2, respectively. The dashed lines 1 and 2 show the Casimir free energy calculated using the simple Drude and plasma models. Similar to Fig. 3, here the Casimir free energy is positive. The distinctions of Fig. 4 from Fig. 3(a) are, however, not of only quantitative character. Thus, for a Ag film on an Al plate the free energies computed using the optical data are larger than the ones computed using the simple Drude and plasma models. For Ag films of 50 and 100 nm thickness the free energies computed using the optical data are larger by the factors of 1.396 and 1.024 if the Drude model is used and by the factors of 1.259 and 1.092 in the case of the plasma model. The Casimir free energies of Ag films of 50 and 100 nm thickness computed using the Drude model approach (the solid line 1) are larger than those computed using the plasma model approach (the solid line 2) by the factors of 1.085 and 10.4, respectively.

V. FILMS WITH VARYING SIGN OF THE CASIMIR FREE ENERGY

In this section we demonstrate that for some pairs of metals the Casimir free energy of a film changes its sign depending on the film thickness. We start from a Au film deposited on a Ag plate. In this case the computational results for the positive Casimir free energy are presented in Fig. 5(a) by the pairs of lines labeled 1 and 2, where all the notations are the same as in Figs. 1–4. For the relatively large film thickness the free energy computed using the Drude model (the solid and dashed lines 1) goes to the classical limit and computed using the plasma model (the solid and dashed lines 2) exponentially fast drops to zero. For Au films of 50 and 100 nm thickness the free energy shown by the solid line 1 is by the factors of 36.25 and 135.9 larger than that shown by the solid line 2, respectively. Similar to Figs. 1–4 the role of the optical data is more pronounced for the free energy computed using the plasma model approach.

For the smallest film thicknesses Fig. 5(a), however, differs from all the above figures. Here, the dashed lines 1 and 2 computed using the simple Drude and plasma models deviate considerably from the solid lines 1 and 2 computed using the optical data. The latter lines approach to their maximum values. Because of this, it is interesting to calculate the Casimir free energy for thinner Au films in the range from 10 to 20 nm, where the role of optical data becomes dominant. In Fig. 5(b) the computational results for $\mathcal{F}$ multiplied by the second power of the film thickness are shown by the solid lines 1 and 2 computed using the optical data extrapolated by the Drude and plasma models, respectively. As is seen in Figs. 5(a,b), the maximum values of $\mathcal{F}$ are reached for films of 19 and 21 nm thickness when the Drude and plasma model approaches are used in computations, respectively. From Fig. 5(b) it is seen that with decreasing film thickness the Casimir free energy decreases and takes the zero value for $a \approx 14.2$ and 16.1 nm for the Drude and plasma model approaches, respectively. For thinner films the Casimir free energy changes its sign from plus to minus, i.e., the respective Casimir pressure becomes attractive from repulsive. If for some film thickness the free energy predicted by one of the calculation approaches is almost zero, a discrepancy between the predicted values increases. Thus, for Au films of 14 and 16 nm thickness the magnitudes of the free energy calculated using the Drude and plasma model approaches differ by the factors of 11.8 and 18.0, respectively.

It is also possible to get the positive free energy (i.e., the Casimir repulsion) for very thin

films and change its sign for the negative one with increasing film thickness. For this purpose one can use Ag films deposited on a Au plate. In Fig. 6(a) the magnitude of the negative Casimir free energy of a Ag film on a Au plate is plotted as a function of the film thickness using the same notations as in all previous figures. For the films of 50 and 100 nm thickness the magnitude of the free energy computed by the Drude model approach (the solid line 1) is larger than that computed by the plasma model approach (the solid line 2) by the factors of 46.8 and 245.9, respectively. Again, with decreasing film thickness the dashed lines 1 and 2 computed using the simple Drude and plasma models deviate significantly from the solid lines 1 and 2 which approach to their maximum values reached for $a = 20$ and 23 nm, respectively.

In Fig. 6(b) we plot the Casimir free energy of a Ag film on a Au plate computed using the Drude and plasma model approaches for film thicknesses in the range from 10 to 25 nm. In order to use the natural scale, the quantity $a^2\mathcal{F}$ is plotted rather than $\mathcal{F}$. As is seen in Fig. 6(b), the Casimir free energies computed using the Drude and plasma model approaches take the zero value for films of approximately 14.8 and 17.5 nm thickness, respectively. For thinner Ag films the Casimir free energy changes its sign and becomes positive, which correspond to the Casimir repulsion. For Ag films of 15 and 18 nm thickness the magnitudes of the Casimir free energy predicted by the Drude and plasma model approaches are different by the factors of 9.6 and 8.4, respectively.

VI. CONCLUSIONS AND DISCUSSION

In the foregoing we have investigated the Casimir free energies and pressures of metal films deposited on metallic plates made of different metals. It is shown that this configuration possesses unusual properties which are significantly different from the well studied case of two metallic plates interacting through a vacuum gap. These properties shed new light on an unresolved problem in Casimir physics, the so-called Casimir puzzle, and are also interesting for applications because the van der Waals and Casimir forces play an important role in the stability of thin films.

Specifically, we have shown that the Casimir free energy of metal films of a few tens nanometer thickness deposited on a metallic plate differs widely depending on whether the Drude or the plasma model approach is employed in calculations. Depending on metals

used this difference can reach hundreds and even thousands of percent, so that it can be easily discriminated experimentally. One more qualitative result is that the free energy of a metal film on a metallic plate reaches the classical limit with increasing film thickness only if the Drude model approach is used in computations. This limit is achieved for unusually small film thickness of about 150 nm. As a result, in the limiting case of an ideal metal the Casimir free energy of a metal film does not vanish in contradiction with the fact that electromagnetic fluctuations cannot penetrate in its interior. If the film and plate metals are described by the plasma model approach, the Casimir free energy of a film drops to zero exponentially fast and there is no classical limit.

We have performed numerical computations of the Casimir free energy and pressure of Ag and Au films deposited on Cu and Al plates using the Drude and plasma model approaches. It is shown that for a Cu plate the Casimir free energy and pressure of Ag and Au films are negative and correspond to the Casimir attraction, whereas for an Al plate they are positive and correspond to the Casimir repulsion. For a Au film deposited on a Ag plate and for a Ag film deposited on a Au plate the Casimir free energy changes its sign from minus to plus and from plus to minus, respectively, with increasing film thickness. All computations have been made in two different ways: using the complete optical data for the complex index of refraction of the film and plate metals extrapolated to zero frequency by the Drude and plasma models and by using the simple Drude and plasma models at all frequencies. According to our results, in the framework of the Drude model approach the optical data influence the Casimir free energy and pressure of thin metal films, and this influence quickly decreases for films from 50 to 100 nm thickness depending on the film and plate metals. If the plasma model approach is used in computations, the optical data affect considerably the obtained values of the free energy and pressure for any film thickness.

To conclude, the configuration of metal films deposited on metallic plates display several unusual properties of the Casimir free energy and pressure which makes it interesting for various applications in both fundamental physics and in surface science.

[1] V. A. Parsegian, *Van der Waals Forces: A Handbook for Biologists, Chemists, Engineers, and Physicists* (Cambridge University Press, Cambridge, 2005).

[2] M. Bordag, G. L. Klimchitskaya, U. Mohideen, and V. M. Mostepanenko, *Advances in the Casimir Effect* (Oxford University Press, Oxford, 2015).

[3] J. F. Babb, G. L. Klimchitskaya, and V. M. Mostepanenko, Phys. Rev. A **70**, 042901 (2004).

[4] A. O. Caride, G. L. Klimchitskaya, V. M. Mostepanenko, and S. I. Zanette, Phys. Rev. A **71**, 042901 (2005).

[5] H. Safari, D.-G. Welsch, S. Y. Buhmann, and S. Scheel. Phys. Rev. A **78**, 062901 (2008).

[6] J. M. Obrecht, R. J. Wild, M. Antezza, L. P. Pitaevskii, S. Stringari, and E. A. Cornell, Phys. Rev. Lett. **98**, 063201 (2007).

[7] M. Chaichian, G. L. Klimchitskaya, V. M. Mostepanenko, and A. Tureanu, Phys. Rev. A **86**, 012515 (2012).

[8] F. Chen, U. Mohideen, G. L. Klimchitskaya, and V. M. Mostepanenko, Phys. Rev. A **74**, 022103 (2006).

[9] S. de Man, K. Heeck, and D. Iannuzzi, Phys. Rev. A **82**, 062512 (2010).

[10] G. Gómez-Santos, Phys. Rev. B **80**, 245424 (2009).

[11] P. J. van Zwol, G. Palasantzas, and J. Th. M. De Hosson, Phys. Rev. B **77**, 075412 (2008).

[12] D. Drosdoff and L. M. Woods, Phys. Rev. A **84**, 062501 (2011).

[13] H. B. Chan, V. A. Aksyuk, R. N. Kleiman, D. J. Bishop, and F. Capasso, Science **291**, 1941 (2001).

[14] E. Buks and M. L. Roukes, Phys. Rev. B **63**, 033402 (2001).

[15] J. Zou, Z. Marcet, A. W. Rodriguez, M. T. H. Reid, A. P. McCauley, I. I. Kravchenko, T. Lu, Y. Bao, S. G. Johnson, and H. B. Chan, Nature Commun. **4**, 1845 (2013).

[16] G. L. Klimchitskaya, U. Mohideen, and V. M. Mostepanenko, Rev. Mod. Phys. **81**, 1827 (2009).

[17] A. W. Rodriguez, F. Capasso, and S. G. Johnson, Nature Photon. **5**, 211 (2011).

[18] E. M. Lifshitz and L. P. Pitaevskii, *Statistical Physics*, Part II (Pergamon, Oxford, 1980).

[19] R. S. Decca, E. Fischbach, G. L. Klimchitskaya, D. E. Krause, D. López, and V. M. Mostepanenko, Phys. Rev. D **68**, 116003 (2003).

[20] R. S. Decca, D. López, E. Fischbach, G. L. Klimchitskaya, D. E. Krause, and V. M. Mostepanenko, Ann. Phys. (N. Y.) **318**, 37 (2005).

[21] R. S. Decca, D. López, E. Fischbach, G. L. Klimchitskaya, D. E. Krause, and V. M. Mostepanenko, Phys. Rev. D **75**, 077101 (2007).

[22] R. S. Decca, D. López, E. Fischbach, G. L. Klimchitskaya, D. E. Krause, and V. M. Mostepanenko, Eur. Phys. J. C **51**, 963 (2007).

[23] C.-C. Chang, A. A. Banishev, R. Castillo-Garza, G. L. Klimchitskaya, V. M. Mostepanenko, and U. Mohideen, Phys. Rev. B **85**, 165443 (2012).

[24] A. A. Banishev, G. L. Klimchitskaya, V. M. Mostepanenko, and U. Mohideen, Phys. Rev. Lett. **110**, 137401 (2013).

[25] A. A. Banishev, G. L. Klimchitskaya, V. M. Mostepanenko, and U. Mohideen, Phys. Rev. B **88**, 155410 (2013).

[26] V. M. Mostepanenko, J. Phys.: Condens. Matter **27**, 214013 (2015).

[27] I. Brevik, S. Å. Ellingsen, and K. A. Milton, New J. Phys. **8**, 236 (2006).

[28] G. L. Klimchitskaya and V. M. Mostepanenko, Contemp. Phys. **47**, 131 (2006).

[29] I. Brevik, J. B. Aarseth, J. S. Høye, and K. A. Milton, Phys. Rev. E **71** 056101 (2005).

[30] V. B. Bezerra, R. S. Decca, E. Fischbach, B. Geyer, G. L. Klimchitskaya, D. E. Krause, D. López, V. M. Mostepanenko, and C. Romero, Phys. Rev. E **73**, 028101 (2006).

[31] V. M. Mostepanenko, V. B. Bezerra, R. S. Decca, E. Fischbach, B. Geyer, G. L. Klimchitskaya, D. E. Krause, D. López, and C. Romero, J. Phys. A: Math. Gen. **39**, 6589 (2006).

[32] W. J. Kim, M. Brown-Hayes, D. A. R. Dalvit, J. H. Brownell, and R. Onofrio, Phys. Rev. A **78**, 020101(R) (2008).

[33] R. S. Decca, E. Fischbach, G. L. Klimchitskaya, D. E. Krause, D. López, U. Mohideen, and V. M. Mostepanenko, Phys. Rev. A **79**, 026101 (2009).

[34] G. Bimonte, Phys. Rev. A **79**, 042107 (2009).

[35] R. O. Behunin, F. Intravaia, D. A. R. Dalvit, P. A. Maia Neto, and S. Reynaud, Phys. Rev. A **85**, 012504 (2012).

[36] R. O. Behunin, D. A. R. Dalvit, R. S. Decca, C. Genet, I. W. Jung, A. Lambrecht, A. Liscio, D. López, S. Reynaud, G. Schnoering, G. Voisin, and Y. Zeng, Phys. Rev. A **90**, 062115 (2014).

[37] G. Bimonte, D. López, and R. S. Decca, Isoelectronic determination of the thermal Casimir force, arXiv:1509.05349v2.

[38] R. S. Decca, Int. J. Mod. Phys. A **31**, 1641024 (2016).

[39] G. Bimonte, Phys. Rev. Lett. **112**, 240401 (2014).

[40] G. Bimonte, Phys. Rev. Lett. **113**, 240405 (2014).

[41] G. Bimonte, Phys. Rev. B **91**, 205443 (2015).

[42] F. Chen, G. L. Klimchitskaya, V. M. Mostepanenko, and U. Mohideen, Phys. Rev. B **76**, 035338 (2007).

[43] C.-C. Chang, A. A. Banishev, G. L. Klimchitskaya, V. M. Mostepanenko, and U. Mohideen, Phys. Rev. Lett. **107**, 090403 (2011).

[44] A. A. Banishev, C.-C. Chang, R. Castillo-Garza, G. L. Klimchitskaya, V. M. Mostepanenko, and U. Mohideen, Phys. Rev. B **85**, 045436 (2012).

[45] G. L. Klimchitskaya and V. M. Mostepanenko, J. Phys. A: Math. Theor. **41**, 312002 (2008).

[46] V. B. Bezerra, G. L. Klimchitskaya, and V. M. Mostepanenko, Phys. Rev. A **65**, 052113 (2002).

[47] V. B. Bezerra, G. L. Klimchitskaya, and V. M. Mostepanenko, Phys. Rev. A **66**, 062112 (2002).

[48] V. B. Bezerra, G. L. Klimchitskaya, V. M. Mostepanenko, and C. Romero, Phys. Rev. A **69**, 022119 (2004).

[49] G. L. Klimchitskaya and C. C. Korikov, Phys. Rev. A **91**, 032119 (2015); **92**, 029902(E) (2015).

[50] B. Geyer, G. L. Klimchitskaya, and V. M. Mostepanenko, Phys. Rev. D **72**, 085009 (2005).

[51] G. L. Klimchitskaya, B. Geyer, and V. M. Mostepanenko, J. Phys. A: Math. Gen. **39**, 6495 (2006).

[52] G. L. Klimchitskaya, U. Mohideen, and V. M. Mostepanenko, J. Phys. A: Math. Theor. **41**, 432001 (2008).

[53] G. L. Klimchitskaya and C. C. Korikov, J. Phys.: Condens. Matter **27**, 214007 (2015).

[54] G. L. Klimchitskaya and V. M. Mostepanenko, Phys. Rev. A **92**, 042109 (2015).

[55] L. Boinovich and A. Emelyanenko, Adv. Colloid Interface Sci. **165**, 60 (2011).

[56] G. L. Klimchitskaya, U. Mohideen, and V. M. Mostepanenko, J. Phys. A: Math. Theor. **40**, 339 (2007).

[57] *Handbook of Optical Constants of Solids*, ed. E. D. Palik (Academic, New York, 1985).

[58] M. Boström and Bo E. Sernelius, Phys. Rev. B **61**, 2204 (2006).

[59] M. A. Ordal, L. L. Long, R. J. Bell, S. E. Bell, R. R. Bell, R. W. Alexander, Jr., and C. A. Ward, Appl. Opt. **22**, 1099 (1983).

[60] M. A. Ordal, R. J. Bell, R. W. Alexander, Jr., L. L. Long, and M. R. Querry, Appl. Opt. **24**,

4493 (1985).

[61] M. Boström, C. Persson, and Bo E. Sernelius, Eur. Phys. J. B **86**, 43 (2013).

[62] G. L. Klimchitskaya and V. M. Mostepanenko, Phys. Rev. B **92**, 205410 (2015).

[63] M. Boström and Bo E. Sernelius, Phys. Rev. B **62**, 7523 (2006).

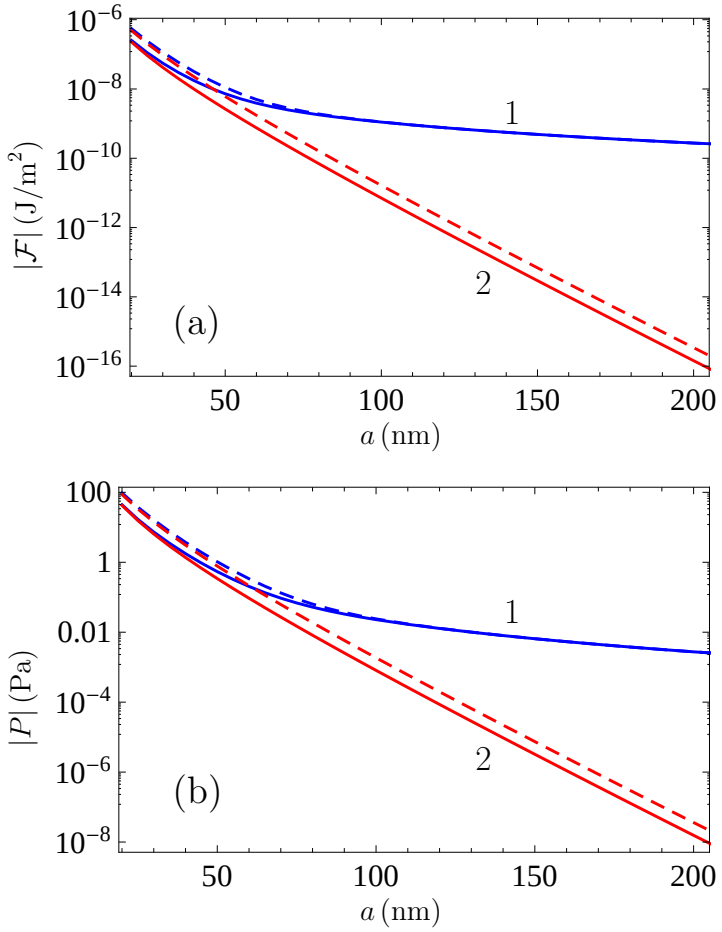


FIG. 1: (Color online) The magnitudes of (a) the Casimir free energy per unit area and (b) the Casimir pressure of a Ag film on a Cu plate computed using the tabulated optical data extrapolated to zero frequency by the Drude (the solid line 1) and plasma (the solid line 2) models are shown as functions of the film thickness. The dashed lines 1 and 2 present the same quantities computed using the simple Drude and plasma models, respectively.

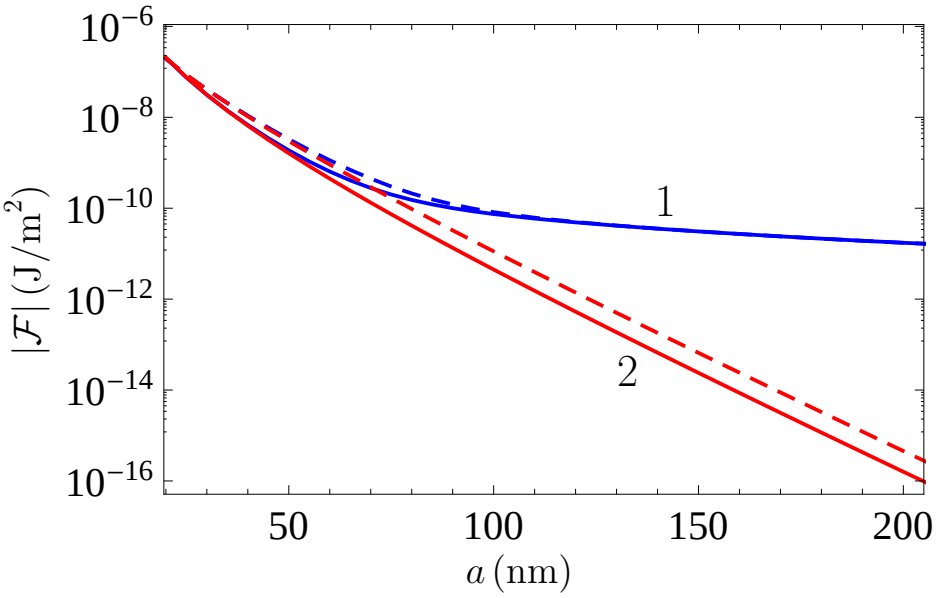


FIG. 2: (Color online) The magnitudes of the Casimir free energy per unit area of a Au film on a Cu plate computed using the tabulated optical data extrapolated to zero frequency by the Drude (the solid line 1) and plasma (the solid line 2) models are shown as functions of the film thickness. The dashed lines 1 and 2 present the same quantities computed using the simple Drude and plasma models, respectively.

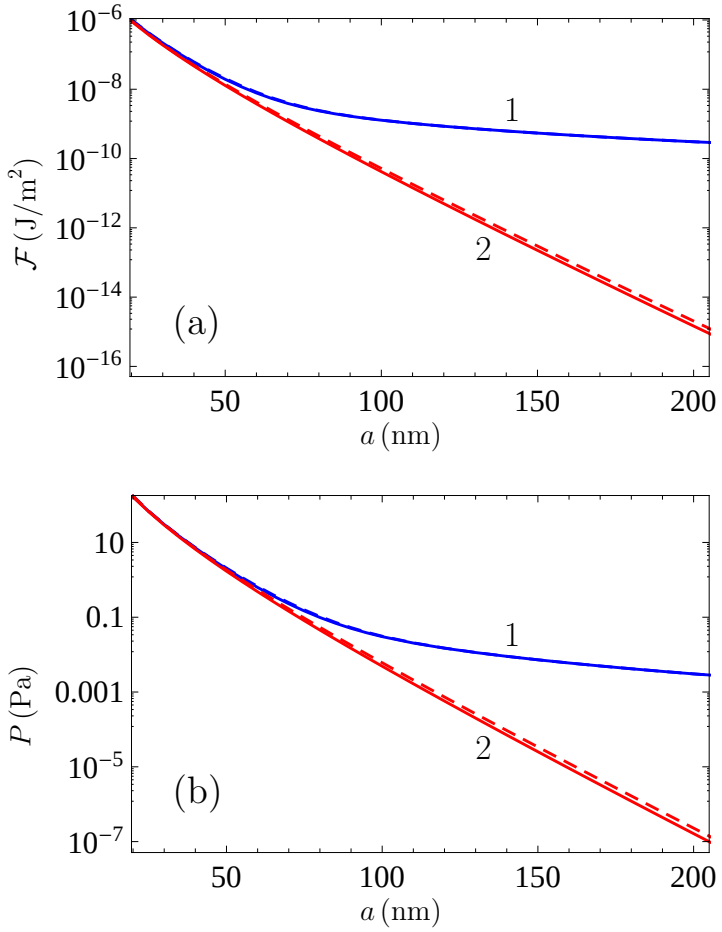


FIG. 3: (Color online) (a) The Casimir free energies per unit area and (b) the Casimir pressures of a Au film on an Al plate computed using the tabulated optical data extrapolated to zero frequency by the Drude (the solid line 1) and plasma (the solid line 2) models are shown as functions of the film thickness. The dashed lines 1 and 2 present the same quantities computed using the simple Drude and plasma models, respectively.

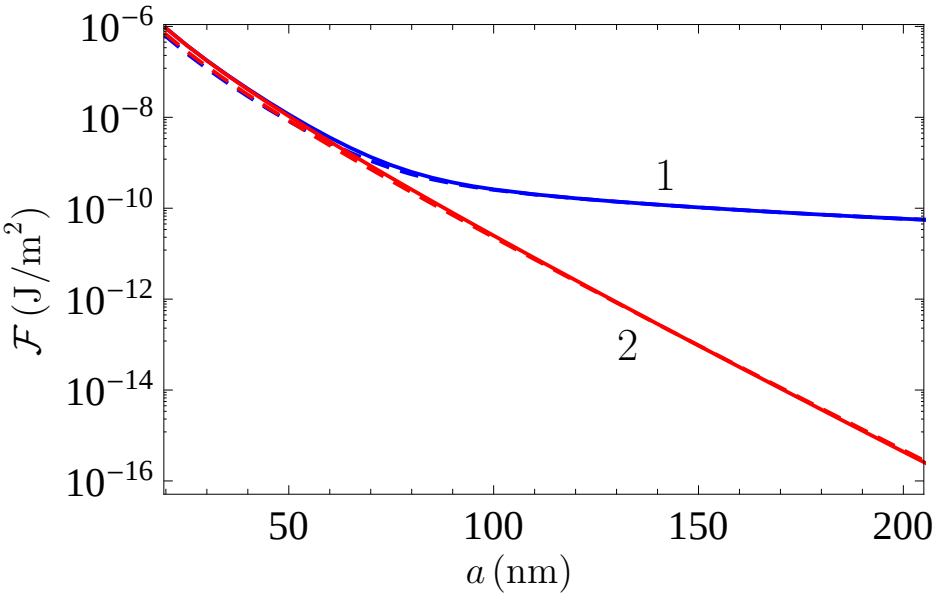


FIG. 4: (Color online) The Casimir free energies per unit area of a Ag film on an Al plate computed using the tabulated optical data extrapolated to zero frequency by the Drude (the solid line 1) and plasma (the solid line 2) models are shown as functions of the film thickness. The dashed lines 1 and 2 present the same quantities computed using the simple Drude and plasma models, respectively.

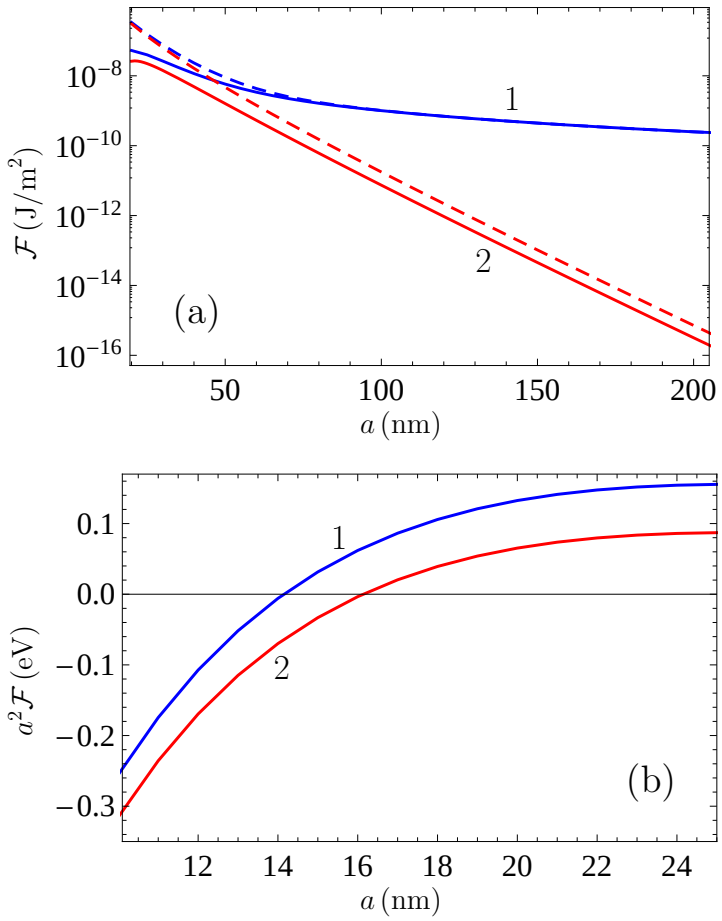


FIG. 5: (Color online) (a) The Casimir free energies per unit area of a Au film on a Ag plate and (b) the same free energies multiplied by the film thickness squared computed using the tabulated optical data extrapolated to zero frequency by the Drude (the solid line 1) and plasma (the solid line 2) models are shown as functions of the film thickness. The dashed lines 1 and 2 present the free energies computed using the simple Drude and plasma models, respectively.

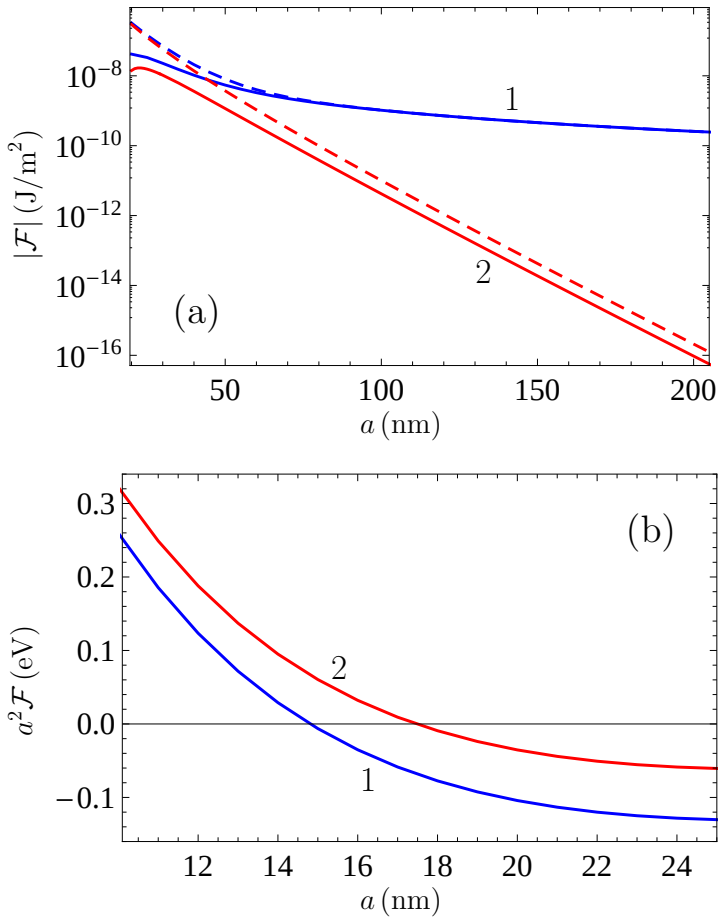


FIG. 6: (Color online) (a) The magnitudes of the Casimir free energy per unit area of a Ag film on a Au plate and (b) the Casimir free energies multiplied by the film thickness squared computed using the tabulated optical data extrapolated to zero frequency by the Drude (the solid line 1) and plasma (the solid line 2) models are shown as functions of the film thickness. The dashed lines 1 and 2 present the magnitudes of the free energies computed using the simple Drude and plasma models, respectively.